CONFERENCE PRE-PRINT

GAM FREQUENCY STRUCTURE AND PROPERTIES IN OHMIC AND POWERFUL ECR-HEATED PLASMAS IN A TOKAMAK

A.V. MELNIKOV 1,2,3

¹ National Research Center "Kurchatov Institute"

Moscow, Russian Federation

² Moscow Institute of Physics and Technology (NRU),

Dolgoprudny, Russian Federation

³ National Research Nuclear University "MEPhI",

Moscow, Russian Federation

E-mail: Melnikov_AV@nrcki.ru

L.G. ELISEEV 1, Ya.M. AMMOSOV 1,2, S.E. LYSENKO 1

¹ National Research Center "Kurchatov Institute"

Moscow, Russian Federation

² Moscow Institute of Physics and Technology (NRU),

Dolgoprudny, Russian Federation

Abstract

The geodetic acoustic mode (GAM) is a high-frequency branch of zonal flows, considered as a mechanism of the turbulence self-regulation, affecting the radial transport of energy and particles. The GAM studies were performed using the heavy ion beam probing (HIBP) of plasma in the T-10 tokamak (R=1.5 m, a=0.3 m, B_t =2.5 T, I_{pl} < 330 kA, deuterium). HIBP measured plasma potential oscillations from the central area to the limiter. It was shown that the GAM has a complex frequency structure consisting of three separate frequency peaks in the power spectral density of plasma potential: the main GAM peak with a frequency of $f_{GAM} \sim 20$ kHz, and two satellite peaks, high-frequency (HF) and low-frequency (LF) ones, shifted from the main peak by the same $\Delta f \sim 4$ kHz. Each of the three GAM peaks has the character of a global eigenmode of plasma oscillations with the frequency and amplitude of potential fluctuations almost constant in a wide radial region from the plasma core to the edge. At the edge, the amplitude of the GAM peaks decreases to zero at the plasma boundary. The radial dependence of the GAM frequency does not obey the local scaling $f_{\text{GAM}} \sim C_s/R$, where C_s is the ion-sound velocity. Nevertheless, in ohmic discharges, as well as at the moderate power of ECR heating ($P_{EC} < 0.5 \text{ MW}$), the frequencies of each of the three GAM peaks follows the temperature dependence of local scaling with C_s , taken at the outermost point of the constant amplitude. With a further increase in temperature or at powerful ECR heating (0.5 MW < P_{EC} < 2.2 MW), the frequencies of both the main GAM peak and both satellites deviate from the theoretical dependence and saturate. As the power of the ECR-heating (temperature) increases, the frequency difference between the main GAM peak of the HF satellite decreases, and the two peaks merge into the single, reaching the upper limit for f_{GAM} . The bicoherence analysis indicates the three-wave coupling of GAM with plasma turbulence in a wide spectral range up to 350 kHz, including quasicoherent mode with 80 kHz $< f_{QCM} < 300$ kHz and stochastic low frequency mode with fsLF < 50 kHz. Each GAM peak has its own frequency range of coupling.

1. INTRODUCTION

The oscillating radial electric field E_r drives the torsional poloidal oscillations along the magnetic surfaces (zonal flows, ZFs). According to the theory, these oscillations have a toroidal and poloidal wavenumbers m=n=0, the fluctuations of density n_e are weaker than the fluctuations of potential φ , $\Delta n_e/n_e \ll e\Delta\varphi/T_e$. Geodetic acoustic mode (GAM) is a high-frequency branch of zonal flow. The GAM frequency follows the dependence on plasma parameters $f_{GAM} = C_s / \sqrt{2\pi}R$, where C_s is the ion-sound velocity, as predicted by a local theory [1]. The first observations of GAM were carried out on three tokamaks: TEXT [2], DIII-D [3] and T-10 [4, 5]. The general interest to GAM emerges after the review paper, considering both GAMs and low frequency (or residual) ZFs with f_{ZF} of a few kHz, $f_{ZF} < f_{GAM}$ [6]. It has been shown that the GAM is excited as a result of a nonlinear interaction between various spectral components of turbulence, or as an effect of energetic particles (e-GAM). ZF/GAM is considered as a mechanism of the turbulence self-regulation, affecting the radial transport of energy and particles in toroidal fusion devices. Due to that ZF/GAM is considered as a mechanism influencing L-H transitions [7, 8]. Progress in the ZF and GAM researches is described in the reviews [9 - 11].

Experiments have shown that the GAM has a fine structure: in addition to the main peak, a high-frequency satellite is visible on the power spectrum of plasma potential. The presence of the HF-satellite does not fit to the local theory [1]. Recent theoretical analysis considers the formation of the GAM fine structure or appearance of

satellites as a result of nonlinear interaction between GAM and Low Frequency ZF [12, 13]. The further development of this concept is presented in this IAEA-FEC [14, 15].

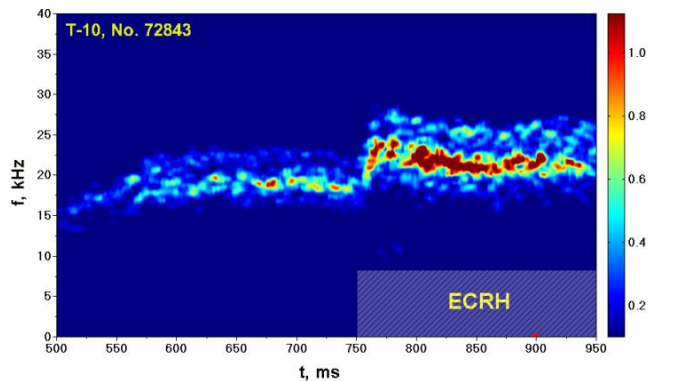
Recent advances in the HIBP diagnostics on the T-10 tokamak increased the signal accuracy, time and spatial resolution [16]. The presented report describes the results of a dedicated study of the GAM frequency fine structure and properties in regimes with ohmic and powerful electron cyclotron resonance heating (ECRH) in the T-10 tokamak. The goal of the work is to check the hypothesis that the HF satellite is another geodetic acoustic mode, which is located in a deeper plasma region with a higher temperature, by the analysis of the main GAM frequency and spatial structure, the dependence of frequency on temperature, and the interaction of the GAM with broadband turbulence. It combines the extended diagnostic capabilities and widening of the temperature domain by exploring the high ECRH power.

2. EXPERIMENTAL SETUP

In the T-10 circular tokamak (toroidal field $B_t = 1.5$ -2.42 T, major and minor radii R = 1.5 m, a = 0.3 m), the advanced heavy ion beam probe (HIBP) diagnostics was used to study GAMs. It measures the fluctuating component of the plasma potential, density, and poloidal component of magnetic potential with a high spatial (~1 cm) and temporal (1 µs) resolution [17, 18]. Tl⁺ ions with an energy of $E_b < 330$ keV probed the plasma from the edge to the core [16]. Deuterium plasma with ohmic and powerful ECR heating ($P_{EC} < 2.2$ MW) was studied in a wide range of plasma parameters: temperature $T_e < 3.1$ keV, $T_i < 0.6$ keV, density $n_e \sim 0.7$ -4×10¹⁹ m⁻³, current $I_{pl} = 150$ -300 kA. Evolution of the main plasma parameters during the high-power ECRH, as well as the HIBP measurement of mean plasma potential were described in the report at the 28-th IAEA Conference FEC-2020 [19].

3. FREQUENCY AND RADIAL STRUCTURE OF THE GAM

Advanced HIBP diagnostics with improved signal sensitivity allowed us to observe the evolution and fine frequency structure of the GAM. For the first time it was shown that GAM consists of three separated frequency peaks, while previously only two peaks were observed. They are the main GAM peak with f_{GAM} , the HF satellite with $f_{\text{HF_sat}}$ and the LF satellite with $f_{\text{LF_sat}}$, all three peaks are shown in Figs. 1 and 2. Unless the Amplitude of the LF satellite is lower than other peaks by a factor of 2-4, it is clearly visible in potential spectra or spectrogram in the form of the separated peak or a shoulder in the lower-frequency part of spectra.



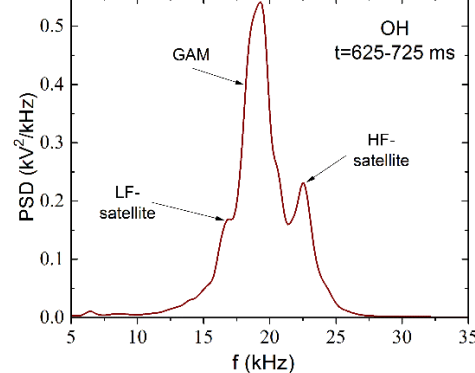


FIG. 1. Spectrogram of plasma potential fluctuations in discharge with OH and ECR-heating: B_t =2.4 T, I_{pl} = 270 kA, $n_e \sim 2$ -3.5×10¹⁹ m^{-3} , P_{EC} = 1.35 MW.

FIG. 2. The fine structure of GAM: main GAM peak, LF, and HF satellites on the power spectral density of potential fluctuations in the ohmic phase of the discharge before the start of ECRH.

As a rule, the frequency differences between the GAM and its satellites are equal to $\Delta f_{\text{HF}} = f_{\text{HF_sat}} - f_{\text{GAM}}$, $\Delta f_{\text{LF}} = f_{\text{GAM}} - f_{\text{LF_sat}}$, $\Delta f_{\text{HF}} = \Delta f_{\text{LF}} = \Delta f$ and they are $\Delta f \sim 4$ kHz. Such a frequency structure of GAM corresponds to a nonlinear model of interaction between GAM and low-frequency ZF, in assumption the ZF frequency, f_{ZF} is equal to Δf [12, 13]. The main peak of the GAM and its satellites dominate the power spectra of the plasma potential in the OH and ECRH stages of discharge. As a rule, the GAM amplitude increases with ECR heating.

The main GAM peak and both satellites have a uniform radial structure with a constant frequency in the wide radial region shown in Fig. 3 (a), that indicates the feature of the global eigenmode of plasma oscillations. In the

present example of OH scenario $f_{\text{GAM}} = 18 \text{ kHz}$, $f_{\text{HF_sat}} = 21 \text{ kHz}$, $f_{\text{LF_sat}} = 15 \text{ kHz}$. The radial distribution of the GAM amplitude is shown in Fig. 3(b). We see that the amplitude of each of the three peaks is different, but it is practically constant over a wide radial range. Approaching to the periphery, the amplitude begins to fall down to the noise level. The plato radial area for the amplitude of the HF satellite, $r \le r_{\text{HF_plato}} = 23 \text{ cm}$, is the narrowest, for the LF satellite it is the widest $r \le r_{\text{LF_plato}} = 27 \text{ cm}$, and for the main GAM peak it is in the middle between them, $r \le r_{\text{GAM_plato}} = 25 \text{ cm}$. The almost constant frequency difference between the three peaks allows us to interpret the HF satellite as the second branch of the GAM, which originated in a deeper region of the plasma with a higher temperature, and the LF satellite as the third branch, originated in an outer region with a lower temperature, while the main GAM peak originates between them.

Following [20], the origin point for each GAM peak was chosen as a radius, where observed GAM frequency, averaged over steady state phase of discharge, coincides with the absolute value of the GAM frequency, $f_{GAM} = C_s / \sqrt{2}\pi R$, where $C_s = \sqrt{(T_e + 7/4T_i)/m}_i$. The origin points for three peaks are taken as $r_{LF_sat} = 29$ cm, $r_{HF_sat} = 25$ cm and $r_{GAM} = 27$ cm. Figure 3 (b) shows that within experimental accuracy origin points are shifted respect to the plato radii about 2 cm and lies about the middle of the slope of the amplitude.

As we mentioned earlier, as a rule, the amplitude of the LF-satellite is significantly (2-4 times) less than the amplitudes of the main GAM peak and the HF-satellite. The amplitudes of each GAM peaks begins to decline monotonously from the origin point to the edge, up to the noise level near the plasma border. The radii of the origin points for each of the peaks are different, but they are fairly constant over a wide range of plasma parameters under study, both in OH and ECRH plasmas.

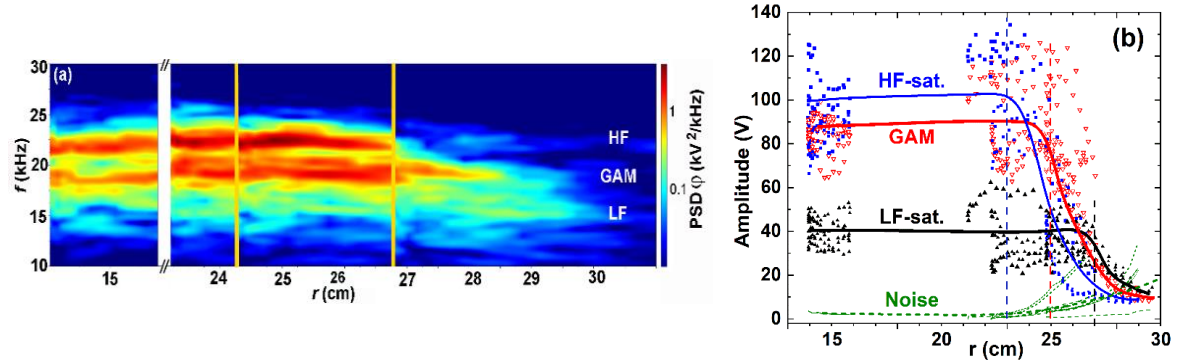


FIG. 3. Typical example of the radial structure of GAM. (a) The frequency for each of the three GAM peaks is constant in the observation area ρ =r/a= 0.55-1.0. (b) Radial distribution of the GAM amplitude. The amplitude of each of the three peaks is constant over a wide radial range. As it approaches the edge, it begins to fall down to the noise level. The region of constant amplitude for the HF satellite is the narrowest, for the LF it is the widest, and for the main peak it is the average between them. OH,

 $B_t = 2.3 \text{ T}, I_{pl} = 230 \text{ kA}, \quad \overline{n_e} \approx 0.6 \text{-} 1 \cdot 10^{19} \text{ m}^{-3}.$

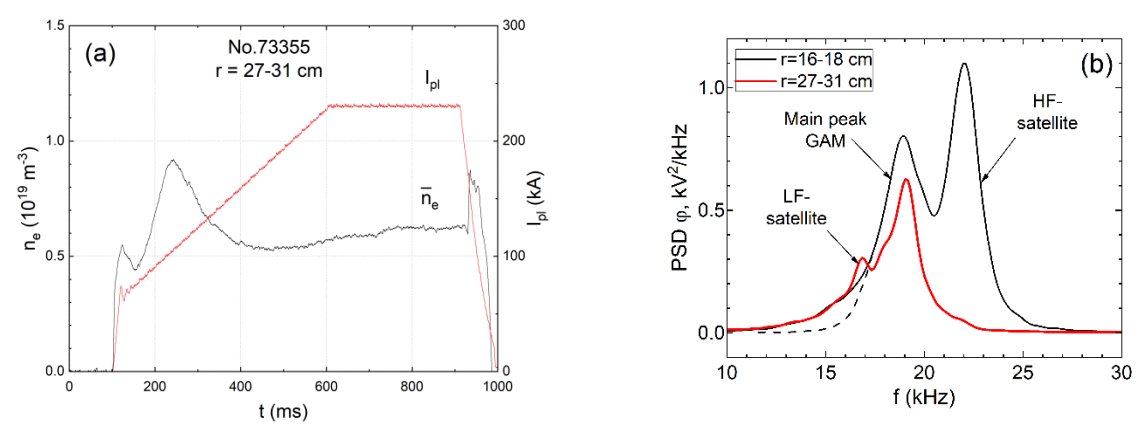


FIG. 4. (a) The evolution of the plasma current I_{pl} and density measured near the core (r=16-18 cm). (b) The spectra of potential fluctuations measured in different observation points. The HF satellite peak is not observed in the outermost observation position.

Figure 4 shows a comparison of the power spectra of potential fluctuations in the core and edge plasmas. It confirms the constancy of the GAM frequency over the radius.

4. DEPENDENCIES OF GAM AND SATELLITES FREQUENCY ON THE TEMPERATURE

In the case of OH and low-power ECRH ($P_{\rm EC}$ < 0.5 MW), all three frequency peaks: the main GAM, LF, and HF satellites have a square root temperature dependence on the value (T_e +7/4 T_i) taken at the points of origin, different for each peak, for $r_{\rm LF_sat}$ = 29 cm, $r_{\rm GAM}$ = 27 cm and $r_{\rm HF_sat}$ = 25 cm. For plasma with powerful ECRH (0.5 MW < $P_{\rm EC}$ < 2.2 MW) or when (T_e +7/4 T_i) at the origin radius $r_{\rm GAM}$ exceeds 0.5 keV, the frequencies of the main GAM peak, as well as LF and HF satellites, deviate from the local theory prediction [1], and the square root dependencies of $f_{\rm GAM}$ on (T_e +7/4 T_i) at $T_{\rm GAM}$ is saturated (Fig. 5). Thus, there is an upper limit for the GAM frequency. The local temperature values are taken at the origin points for each GAM peak.

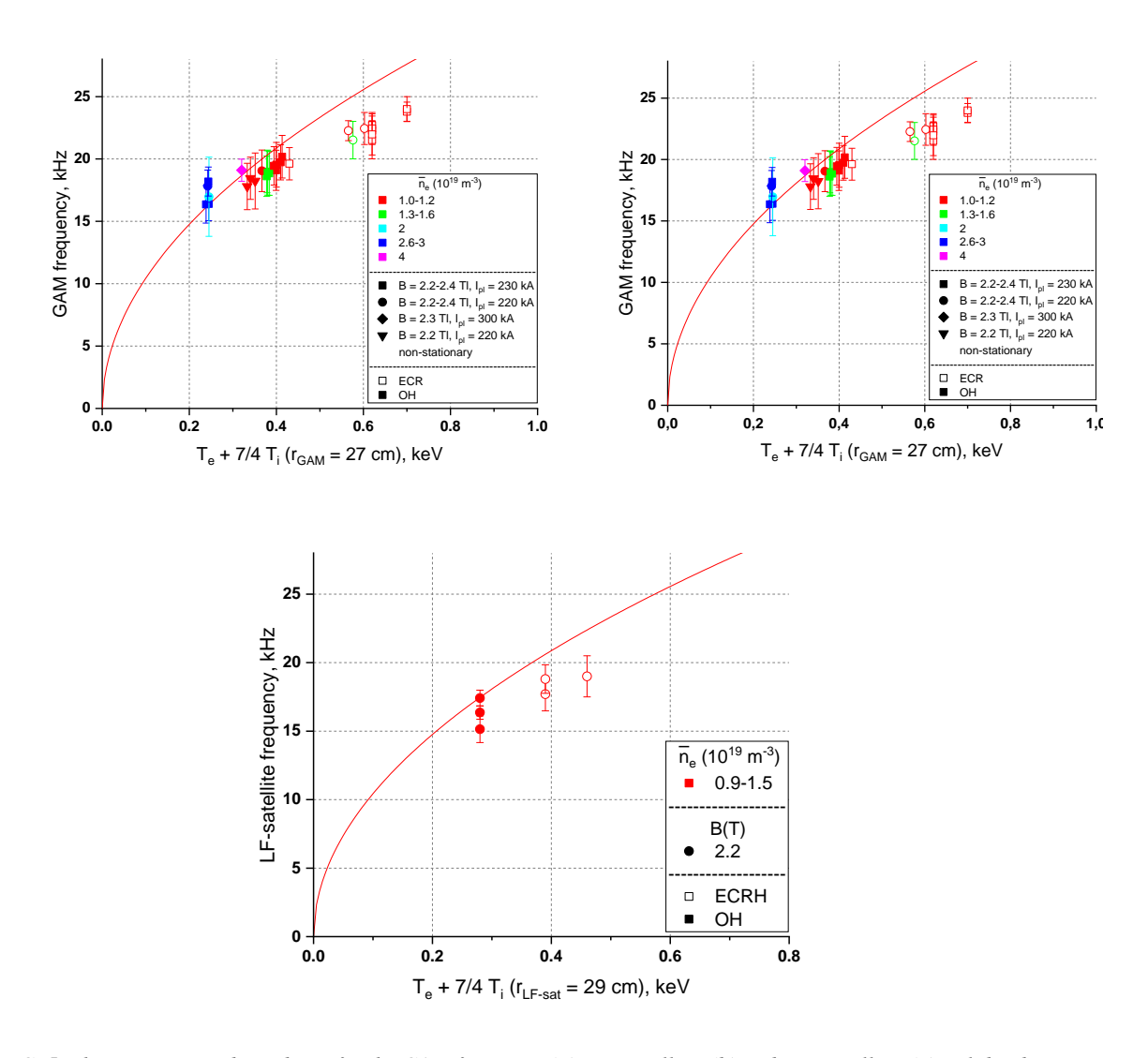


FIG. 5. The temperature dependence for the GAM frequency (a), HF-satellites (b) and LF-satellites (c). solid red curve shows the theoretical $f_{GAM} = C_s / \sqrt{2}\pi R$, where $C_s = \sqrt{(T_e + 7/4T_i)/m}_i$. We consider discharges with ohmic and ECR heating of various power up to the maximum $P_{EC} < 2.2$ MW

Figure 6 shows the frequency difference between GAM and its satellites, Δf_{LF} and Δf_{HF} for the experimental conditions shown in Fig. 5. We see that $\Delta f_{LF} = \Delta f \sim 4$ kHz. When the temperature value $T_e + 7/4T_i$ (r_{GAM})

= 27 cm) approaching 0.7 keV, a systematic decrease in Δf , or convergence of the main GAM and HF satellite peaks is observed up to their complete merging (Fig. 7).

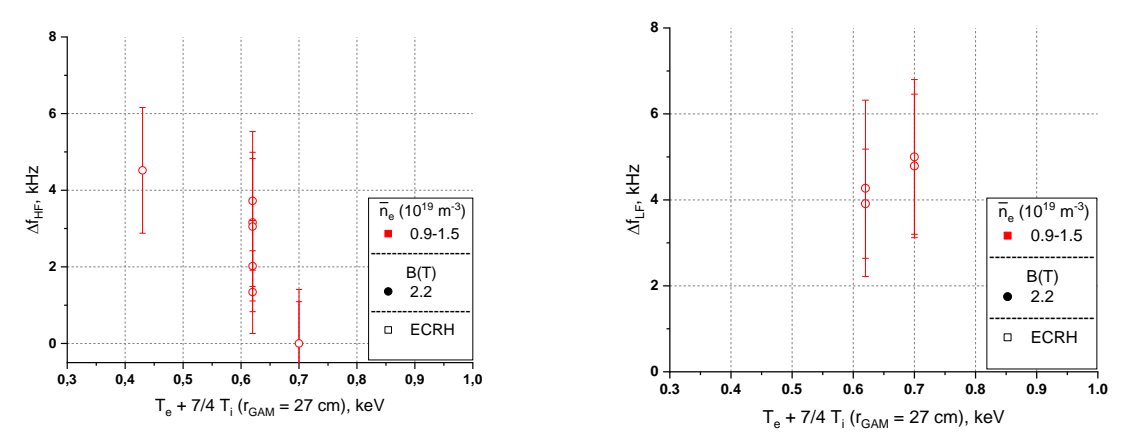


FIG. 6. Frequency difference for GAM peaks, left Δf_{LF} , right - Δf_{HF} . For OH and low-power ECRH, $P_{EC} < 0.5$ MW, the frequency differences are close to each other. When the temperature value Te + 7/4Ti ($r_{GAM} = 27$ cm) approaching 0.7 keV, the merging of the main GAM and HF-satellite peaks takes place.

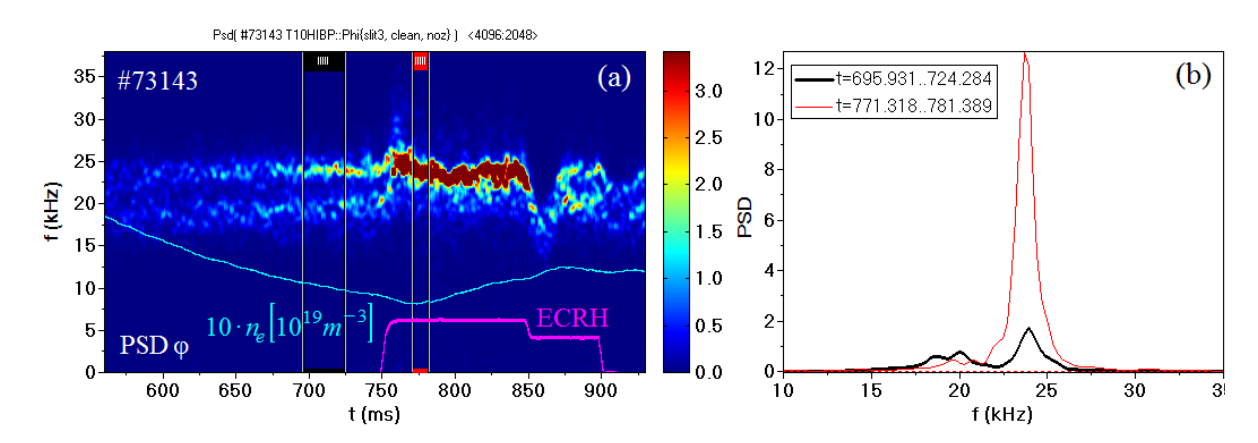


FIG. 7. Merging of the main GAM peak with the satellite during powerful ECRH. (a) Temporal evolution of the potential fluctuation power spectrum, average density (light blue) and ECRH power (purple). (b) Power spectral density before (OH-phase, black) and after (ECRH - phase, red curve) merging.

Note the higher intensity of the merged GAM + HF-satellite peak (red curve) in powerful ECRH phase compared to each of them in OH phase (black curve).

5. INTERACTION OF GAM WITH BROADBAND TURBULENCE

We use the bispectral analysis to study the interaction of GAM with turbulence [10, 20]. The three-wave interaction is described by the bicoherence coefficient b and biphase θ :

$$\begin{split} b_{x,y,z}^2(f_1,\,f_2) &= \frac{|<\Phi_x(f_1)\Phi_y(f_2)\Phi_z^*(f_1+f_2)>|^2}{<|\Phi_x(f_1)\Phi_y(f_2)|^2><|\Phi_z(f_1+f_2)|^2>}, \quad 0 < b_{x,y,z}^2(f_1,\,f_2) < 1 \\ \theta_{x,y,z}(f_1,\,f_2) &= \mathrm{arctg} \frac{Im<\Phi_x(f_1)\Phi_y(f_2)\Phi_z^*(f_1+f_2)>}{Re<\Phi_x(f_1)\Phi_y(f_2)\Phi_z^*(f_1+f_2)>}, \quad -\pi < \theta < \pi. \end{split}$$

A statistically significant b^2 and a finite (non-stochastic) biphase indicate the presence of a three-wave interaction between GAM and turbulence at frequencies f_1 , f_2 , f_1+f_2 [22]. Three-wave interaction characterizes nonlinear

media, it occurs in various fields of physics and engineering. For example, in hydrodynamic turbulence described by the Navier-Stokes equation, a quadratic nonlinearity arises – the Reynolds stresses.

Bispectral analysis indicates a three-wave interaction for each of the three GAM peaks with background turbulence in a wide frequency band from 0 < f < 330 kHz, that is, in the range of quasicoherent modes. Each GAM peak has its own characteristic frequency range of interaction, including a low-frequency quasi-coherent (LFQC) mode, a high-frequency quasicoherent (HFQC) mode, and a stochastic low-frequency (SLF) mode. An example of the $b^2(\varphi, I_{\text{tot}}, I_{\text{tot}})$ for shot No. 72287 is shown in Fig. 8. The signal of the total HIBP current I_{tot} represents the local plasma density. Figure 8 means that the QCM frequencies f_1^{QC} and f_2^{QC} follows the coupling with GAM as $f_1^{\text{QC}} = f_2^{\text{QC}} + f_{\text{GAM}}$.

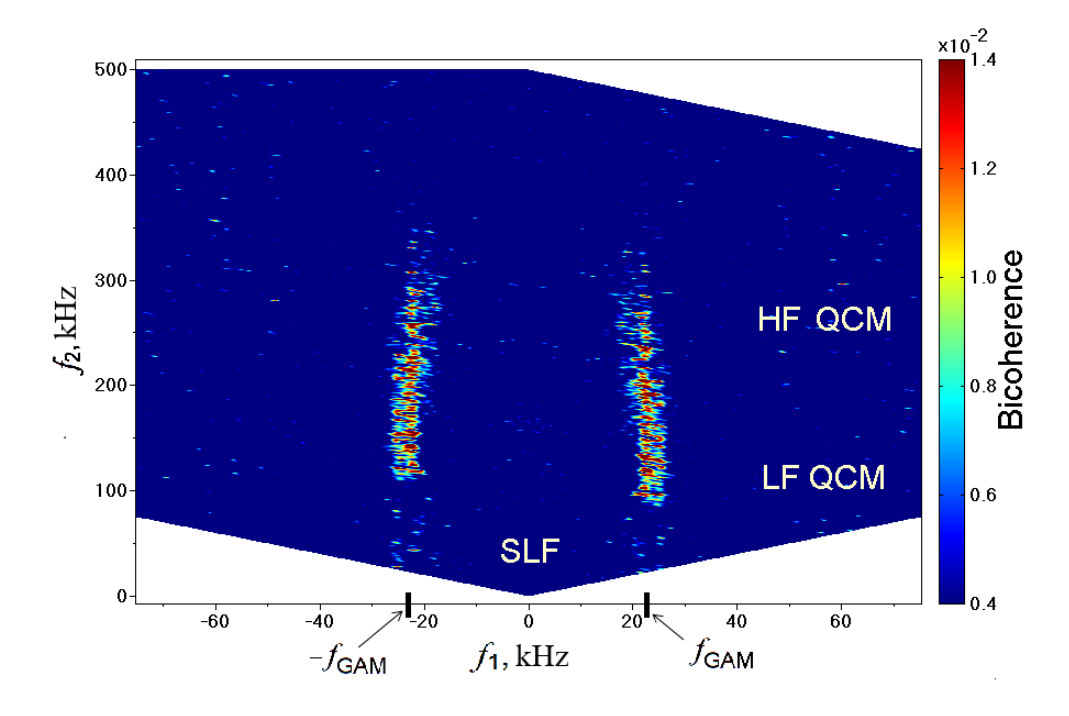


FIG. 8. Three-wave interaction between GAM and turbulence. A statistically significant quadratic bicoherence coefficient indicates the presence of a three-wave interaction between the GAM and LF + HF QCM frequencies; shot No. 72287, OH, $n_e \sim 0.7 \times 10^{19} \text{ m}^{-3}$.

Figure 9 is the zoomed picture of Fig. 8, which shows details of the interaction between GAM and satellites with SLF and QCM in the wide frequency range from 0 to 330 kHz [23].

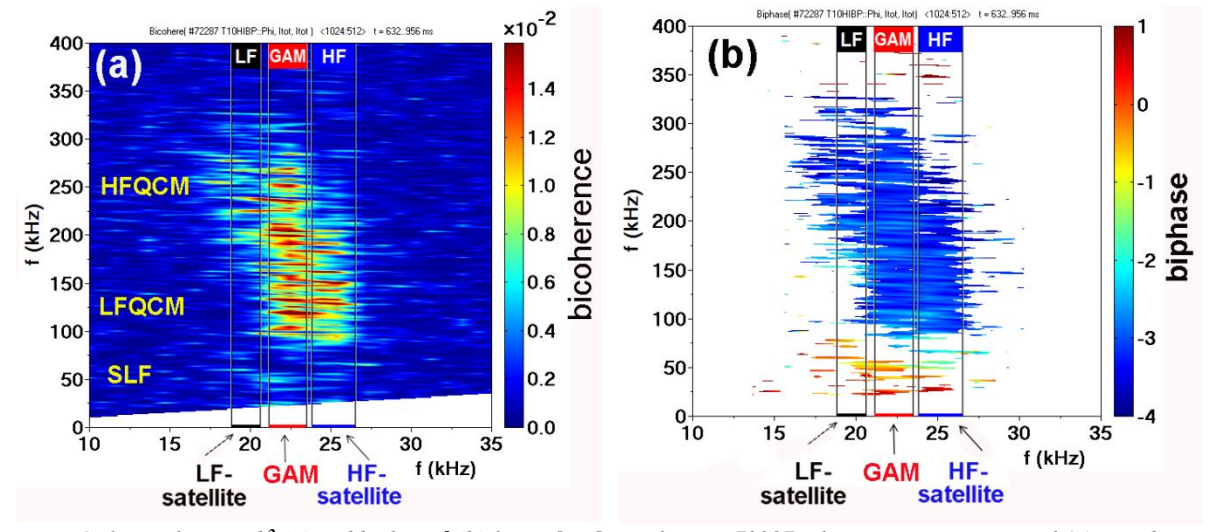


FIG. 9. Bicoherence b² (a) and biphase θ (b) for φ, I_{tot}, I_{tot} in shot No. 72287. Three-wave interaction of GAM and satellites with SLF, QCM is observed in a wide frequency range from 0 to 330 kHz.

Figure 10 shows the dependence of the biphase and the quadratic coefficient of bicoherence on the frequency. The biphase is taken within the range ($-2\pi+1$, 1) to avoid the phase jumps. Figures 9 and 10 show that each of the three branches of GAM has its own intervals of intensive interactions: for GAM with LF+HF QCM: 100 - 330 kHz; for LF satellite with HF QCM: 150 - 330 kHz; and for HF satellite with LF QCM: 100 - 250 kHz. Accordingly, the biphases for GAM and satellites with QCM are: $\theta_{GAM} = -3.1 \pm 0.3$; $\theta_{LF_sat} = -3.1 \pm 0.3$; $\theta_{HF_sat} = -3.1 \pm 0.3$ and for GAM and satellites with SLF, $\theta_{GAM} = 0 \pm 0.5$; $\theta_{LF_sat} = 0 \pm 0.5$; $\theta_{HF_sat} = 0 \pm 0.5$.

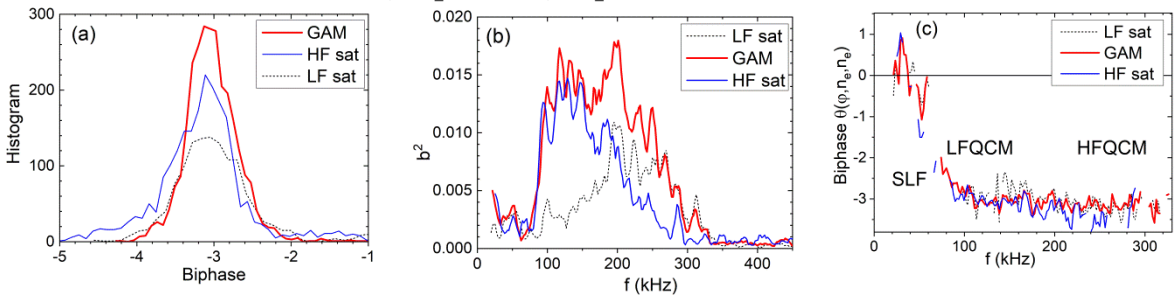


FIG. 10. Interaction of GAM and satellites with turbulence. The dependence of the biphase and the quadratic coefficient of bicoherence on frequency. (a) the histogram for the biphase in interactions with QCM has a maximum of about 2π ; (b) the bicoherence for interactions with QCM; (c) the biphase spectrum for interactions with various types of turbulence.

CONCLUSIONS

We found that GAM has not only HF, but also an LF satellite. Thus, the GAM consists of three separate frequency peaks: the main GAM peak, the HF satellite, and the LF satellite.

As a rule, the amplitude of the LF satellite is significantly (2-4 times) lower than the amplitudes of the main peak and HF satellite. Thus, the theoretical analysis of the GAM frequency structure presented in [12, 13] requires further development and clarification.

For plasma with ohmic and low-power ECR heating ($P_{EC} < 0.5$ MW), all three GAM peaks: the main, LF, and HF satellites have a square root temperature dependence of their frequencies typical for GAM.

A three-wave interaction of all three GAM frequency peaks with turbulence in the wide frequency band from 0 to 330 kHz (stochastic low frequency mode and quasicoherent modes, both LF and HF) has been detected. Each GAM peak has its own typical frequency range of interaction.

The almost constant frequency difference between the three peaks makes it possible to interpret the HF satellite as the second geodetic acoustic mode, born in a deeper region of plasma with a higher temperature, and the LF satellite as the third GAM, born in an outer region with a lower temperature.

For plasma with high-power ECR heating, $0.5 \text{ MW} < P_{EC} < 2.2 \text{ MW}$, the frequencies of the main GAM peak, as well as LF and HF satellites deviate from the prediction of the local theory, the square root dependence of the frequency on temperature f(T) goes into saturation. Thus, an upper frequency limit for GAM has been found.

In this parameter range, with an increase in the ECRH power (temperature), the frequencies of the main peak and HF satellite merge into the single peak.

These new experimental facts require additional theoretical analysis.

ACKNOWLEDGEMENTS

This work was carried out within the State assignment for the National Research Center "Kurchatov Institute". The authors thank the T-10 team, as well as M.A. Drabinskiy, O.D. Krokhalev, F.O. Khabanov and N.K. Kharchev for their help and support. The work of Ya.M. Ammosov and S.E. Lysenko is supported by the Russian Science Foundation, grant 23-72-00042.

REFERENCES

- [1] WINSOR P., JOHNSON J.L., and DAWSON J.M., Geodesic acoustic waves in hydromagnetic systems, Phys. Fluids **11** (1968) 2448.
- [2] SCHOCH P.M., CONNOR K.A., DEMERS D.R. and ZHANG X., Zonal flow measurements using a heavy ion beam probe, Rev. Sci. Instrum. **74** (2003) 1846.
- [3] McKEE G., et al., Observation and characterization of radially sheared zonal flows in DIII-D, Plasma Phys. Control. Fusion **45** (2003) A477–A485.
- [4] MELNIKOV A.V., et al., Observation of the specific oscillations with frequencies near 20 kHz by HIBP, reflectometry and Langmuir probes in T-10, 30th EPS Conf. on Control. Fusion and Plasma Phys., St. Petersburg, 7-11 July 2003, ECA Vol. 27A, P-3.114.
- [5] MELNIKOV A.V., et al., Investigation of geodesic acoustic mode oscillations in the T-10 tokamak, Plasma Phys. Control. Fusion 49 (2006) S87–S110
- [6] DIAMOND P. et al., Zonal flows in plasma—a review, Plasma Phys. Control. Fusion 47 (2005) R35.
- [7] WAGNER F., A quarter-century of H-mode studies, Plasma Phys. Control. Fusion 49 (2007) B1.
- [8] YAN Z. et al., Relating the L-H power threshold scaling to edge turbulence dynamics, Nucl. Fusion 53 (2013) 113038.
- [9] FUJISAWA A. et al., Experimental progress on zonal flow physics in toroidal plasmas, Nucl. Fusion 47 (2007) S718– S726.
- [10] FUJISAWA A., A review of zonal flow experiments, Nucl. Fusion 49 (2009) 013001.
- [11] CONVAY G.D., SMOLYAKOV A.I., and IDO T., Geodesic acoustic modes in magnetic confinement devices, Nucl. Fusion **62** (2022) 013001.
- [12] SOROKINA E.A., Transformation of a geodesic acoustic mode in the presence of a low-frequency zonal flow in a tokamak plasma, JETP Letts. **120** (2024) 642-649.
- [13] LAKHIN V.P., On the nonlinear interaction of geodetic acoustic modes and zonal flows in tokamaks with toroidal plasma rotation, JETP, **168** (2025). In press.
- [14] SOROKINA, E.A., Theoretical model for the experimentally observed GAM's satellites, Proc. 30th IAEA Fusion Energy Conf. (FEC 2025), Chengdu, China, 2025, # 3263.
- [15] ILGISONIS, V.I., SOROKINA, E.A., Nonlinear self-consistent dynamics of geodesic acoustic modes and zonal flows in toroidally rotating tokamak plasmas, Proc. 30th IAEA Fusion Energy Conf. (FEC 2025), Chengdu, China, 2025, # 3268.
- [16] MELNIKOV A.V., KRUPNIK L.I., ELISEEV L.G., et al., Heavy ion beam probing diagnostics to study potential and turbulence in toroidal plasmas, Nucl. Fusion **57** (2017) 072004.
- [17] SERGEEV N.S., MELNIKOV A.V. and ELISEEV L.G., Magnetic component of quasi-coherent mode of plasma fluctuations in ohmic plasma of the T-10 tokamak, JETP Letts. **119** (2024) 852-859.
- [18] MELNIKOV A.V., DRABINSKIY M.A., ELISEEV L.G., et al., Heavy ion beam probe design and operation on the T-10 tokamak, Fusion Eng. and Des. **146**, Part A (2019) 850-853.
- [19] MELNIKOV A.V., et al., Evolution of the electric potential and turbulence in OH and ECRH low-density plasmas at the T-10 tokamak. Proc. 28th IAEA Fusion Energy Conf. (FEC 2020), Rep. EX/5-6.
- [20] MELNIKOV A.V., et al., The features of the global GAM in OH and ECRH plasmas in the T-10 tokamak, Nucl. Fusion **55** (2015) 063001.
- [21] MELNIKOV A.V. et al., Study of interactions between GAMs and broadband turbulence in the T-10 tokamak, Nucl. Fusion **57** (2017) 063001.
- [22] MELNIKOV A.V. et al., GAM and Broadband Turbulence Structure in OH and ECRH Plasmas in the T-10 Tokamak, Plasma and Fusion Research, **13** (2018) 3402109.
- [23] VERSHKOV V.A., MELNIKOV A.V., ELISEEV L.G., Studies of the main components of tokamak plasma turbulence, Plasma Phys. Rep. (submitted).